

Charge neutral fermions and magnetic field driven instability in insulating YbIr_3Si_7

Y. Sato¹, S. Suetsugu¹, T. Tominaga¹, Y. Kasahara¹, S. Kasahara¹, T. Kobayashi¹, S. Kitagawa¹, K. Ishida¹, R. Peters¹, T. Shibauchi², A. H. Nevidomskyy³, L. Qian^{3,4}, J. M. Moya^{3,4}, E. Morosan^{3,4}, and Y. Matsuda¹

¹ *Department of Physics, Kyoto University, Kyoto 606-8502 Japan*

² *Department of Advanced Materials Science, University of Tokyo, Kashiwa, Chiba 277-8561, Japan*

³ *Department of Physics and Astronomy, Rice University, Houston, TX 77005 USA and*

⁴ *Department of Chemistry, Rice University, Houston, TX 77005 USA*

Materials where localized magnetic moments are coupled to itinerant electrons, the so-called Kondo lattice materials, provide a very rich backdrop for strong electron correlations. They are known to realize many exotic phenomena, including unconventional superconductivity, strange metals, and correlated topological phases of matter. Here, we report what appears to be electron fractionalization in insulating Kondo lattice material YbIr_3Si_7 , with emergent neutral excitations that carry heat but not electric current and contribute to metal-like specific heat. We show that these neutral particles change their properties as the material undergoes a transformation between two antiferromagnetic phases in an applied magnetic field. In the low-field AF-I phase, we find that the low temperature linear specific heat coefficient γ and the residual linear term in the thermal conductivity $\kappa/T(T \rightarrow 0)$ are finite, demonstrating itinerant gapless excitations. These results, along with a spectacular violation of the Wiedemann-Franz law, directly indicate that YbIr_3Si_7 is a charge insulator but a thermal metal. Nuclear magnetic resonance spectrum reveals a spin-flop transition to a high field AF-II phase. Near the transition field, γ is significantly enhanced. Most surprisingly, inside the AF-II phase, κ/T exhibits a sharp drop below ~ 300 mK, indicating either opening of a tiny gap or a linearly vanishing density of states. This finding demonstrates a transition from a thermal metal into an insulator/semimetal driven by the spin-flop magnetic transition. These results suggest that spin degrees of freedom directly couple to the neutral fermions, whose emergent Fermi surface undergoes a field-driven instability at low temperatures.

I. INTRODUCTION

Strong electron interactions often lead to the emergence of many-body insulating ground states. Recently, surprising properties have aroused considerable interest in the research of the strongly correlated insulators, SmB_6 and YbB_{12} with simple cubic crystal structures [1]. In these Kondo lattice compounds, the band gap opens up at low temperatures due to the hybridization of localized f -electrons with conduction electrons [2]. In particular, quantum oscillations (QOs) [3–7], specific heat [6, 8, 9], and thermal conductivity [6, 8, 10, 11] experiments have posed a significant paradox, revealing gapless excitations in the bulk, in apparent contradiction with the charge gap seen in transport measurements. While the angular dependence of the QO frequencies suggests a three-dimensional (3D) bulk Fermi surface in SmB_6 [4] and YbB_{12} [5], both materials remain robustly insulating to very high magnetic fields. (In SmB_6 , a 2D Fermi surface has also been reported [3, 12]). Various theoretical models of the QOs in these insulators have been proposed so far [13–22]. Another striking aspect is a nonzero low temperature linear specific heat coefficient $\gamma \sim 10$ mJ/K²mol for SmB_6 [6] and ~ 4 mJ/K²mol for YbB_{12} [8, 9] in zero field. As the specific heat is measured in the bulk insulating state, these results indicate the existence of gapless and charge-neutral excitations in the bulk consistent with an emergent Fermi surface of neutral fermions.

However, there are distinct differences in the gapless excitations in these correlated insulators. In SmB_6 , the

QOs are observed only in the magnetization (de Haas-van Alphen, dHvA, effect). The dHvA oscillations strongly deviate below 1 K from the Lifshitz-Kosevich theory, which is based on Fermi liquid theory [4]. In contrast, in YbB_{12} , the QOs are observed not only in the magnetization, but also in the resistivity (Shubnikov-de Haas, SdH, effect) and both dHvA and SdH oscillations obey the Lifshitz-Kosevich theory down to 50 mK [5]. Moreover, in YbB_{12} , a finite residual temperature-linear (T -linear) term in the thermal conductivity $\kappa_0/T \equiv \kappa/T(T \rightarrow 0)$ is observed, demonstrating the presence of gapless and itinerant neutral fermions [8]. On the other hand, κ_0/T in SmB_6 has been controversial. While κ_0/T of SmB_6 has been reported to be very small but finite [6], the absence of κ_0/T has been reported in [10, 11].

A fascinating question is whether the QOs have any relationship to the neutral fermions. It has been shown that κ_0/T depends on magnetic fields in YbB_{12} , suggesting that the neutral fermions can couple to magnetic fields [8]. Various theoretical models that invoke novel itinerant low-energy neutral excitations within the charge gap that can produce QO signals have been proposed, including Majorana Fermi liquids [17, 18, 22] and a spin liquid with spinon Fermi surface [15, 16]. However, the nature of the neutral fermions is largely elusive and continues to be hotly debated. As the Kondo hybridization between magnetic moments and conduction electrons is the origin of the charge gap formation in these insulators, it is crucially important to clarify how the neutral fermions couple to the magnetic degrees of freedom. Thus, more systematic investigations on a new class of materials are

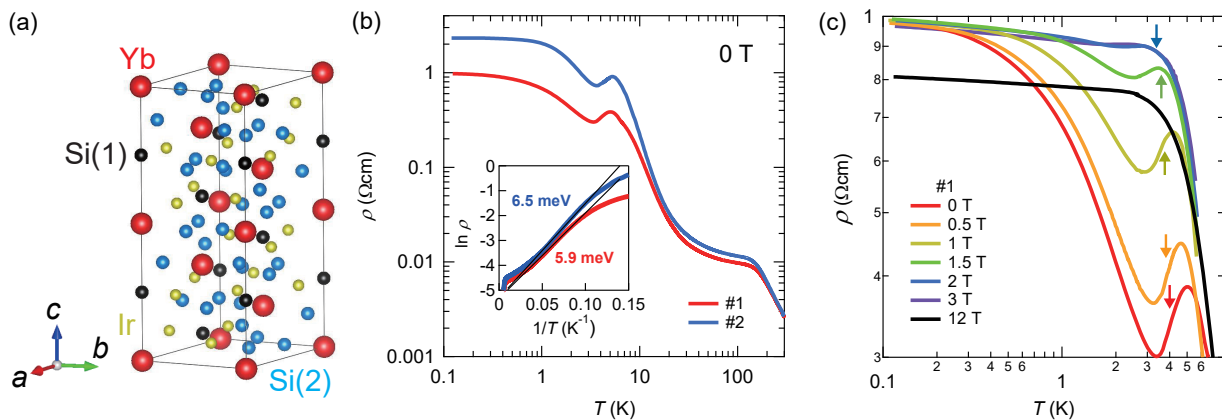


FIG. 1: (a) Crystal structure of YbIr₃Si₇. There are two crystallographically inequivalent Si sites, Si(1) and Si(2). (b) Temperature dependence of the in-plane resistivity ρ for #1 and #2 single crystals. The inset shows the Arrhenius plot of $\ln(\rho)$ versus $1/T$. The solid lines represent the thermally activated behaviors with charge gaps of 5.9 and 6.5 meV for #1 and #2 single crystals, respectively. (c) Low temperature resistivity of #1 crystal in magnetic fields applied perpendicular to the ab plane. The arrows indicate the Néel temperature determined by the specific heat.

highly desired to clarify the relationship between QOs, charge-neutral fermions, and magnetic properties.

Recently a new insulating Kondo lattice compound YbIr₃Si₇ has been discovered [23]. YbIr₃Si₇ has a trigonal ScRh₃Si₇-type crystal structure (Fig. 1(a)). The magnetization and neutron diffraction data show that Yb-ions are very close to the trivalent state in the bulk [23]. In zero field, antiferromagnetic (AFM) order occurs below the Néel temperature $T_N = 4.0$ K. Neutron diffraction measurements report [23] that, in the AFM state corresponding to the Γ_1 state, all the Yb³⁺ moments are oriented along the crystallographic c axis ([001]). Each Yb³⁺ moment is aligned anti-parallel with its six nearest neighbors in the nearly cubic Yb sublattice and parallel with its co-planar next nearest neighbors. The ordered moment is $\sim 1.5 \mu_B/\text{Yb}^{3+}$. We note that in YbIr₃Si₇, the number of free charge carriers has been suggested to be much fewer than the number of local moments [23]. It has therefore been proposed [23] that the system becomes insulating at low temperatures as all the free carriers are consumed in the formation of Kondo singlets. Thus YbIr₃Si₇ has insulating bulk and long-range magnetic correlations, and is distinct from other simple Kondo insulators, such as SmB₆ and YbB₁₂. Interestingly, thickness analysis of the electric transport shows that YbIr₃Si₇ harbours conducting surface states whose origin is however not topological but rather has to do with the valence change to Yb²⁺ near the sample surface [23].

In this paper, we investigate the low-energy excitations in the AFM insulating state of YbIr₃Si₇ by the low-temperature specific heat and thermal conductivity measurements. We find that both γ and κ_0/T are finite at low fields, demonstrating the presence of mobile and gapless excitations of neutral fermions in the bulk insulating state, i.e. YbIr₃Si₇ is a charge insulator but a thermal metal. The AFM order of this compound can

be widely tuned by the external magnetic fields. More precisely, the charge-neutral quasiparticle excitations are either gapless or gapped with an extremely small excitation energy gap, much smaller than the base temperature 90 mK of our thermal conductivity measurements. Most surprisingly, a spin-flop transition from AF-I to AF-II phase at $\mu_0 H \approx 2.5$ T gives rise to an opening of a tiny gap or a linearly vanishing density of states (DOS) of neutral fermions, indicating a transition from a thermal metal into an insulator/semimetal. These results suggest that spin degrees of freedom directly couple to the neutral fermions, whose emergent Fermi surface undergoes a transformation in applied field.

II. MAGNETIC PHASES

A. Resistivity

Figure 1(b) depicts the T -dependence of the in-plane resistivity ρ of YbIr₃Si₇ single crystals (#1 and #2) plotted on a log-log scale. At $T \sim 150$ K, $\rho(T)$ changes its slope, which is attributed to the onset of Kondo correlations. Below ~ 150 K, $\rho(T)$ increases rapidly with decreasing T . As shown in the inset of Fig. 1(b), $\rho(T)$ increases exponentially as $\rho(T) \propto \exp(\Delta_c/k_B T)$ with the charge gap $\Delta_c \sim 5.9$ and ~ 6.5 meV for sample #1 and #2, respectively. At around T_N , $\rho(T)$ is suppressed and increases again with decreasing T down to ~ 0.3 K. Upon further reducing the temperature, $\rho(T)$ saturates down to the lowest temperature. Figure 1(c) depicts the low-temperature resistivity in magnetic field applied parallel to the c axis ($\mathbf{H} \parallel c$). The suppression of $\rho(T)$ at T_N is reduced in magnetic field and is absent above $\mu_0 H = 3$ T, consistent with the previously reported data [23].

It has been shown that the low-temperature saturation of $\rho(T)$ arises from the surface state [23]. In fact,

the difference of the saturation values of ρ between crystals #1 ($\sim 1 \Omega\text{cm}$) and #2 ($\sim 2.1 \Omega\text{cm}$) can be quantitatively explained by the area and thickness of the crystal planes used for the measurements. Similar phenomena have been reported in SmB_6 and YbB_{12} , in which the metallic conductivity takes place at the surfaces of the crystal, while electronic transport and optical measurements clearly show the opening of a finite charge-gap in the bulk at low temperatures. These metallic surface in SmB_6 and YbB_{12} has been attributed to the topological insulating properties at low temperatures [24]. In fact, the metallic surface states have been resolved by angle-resolved photoemission spectroscopy (ARPES) [25, 26]. In particular, spin-ARPES experiments in SmB_6 have revealed the spin-momentum locking of the surface quasiparticles as expected from topologically protected Dirac cones [25]. In YbIr_3Si_7 , on the other hand, the recent photoemission spectroscopy measurements revealed that the surface conduction originates from a change of valence from Yb^{+3} in the bulk to Yb^{+2} on the surface, without invoking topological arguments [23].

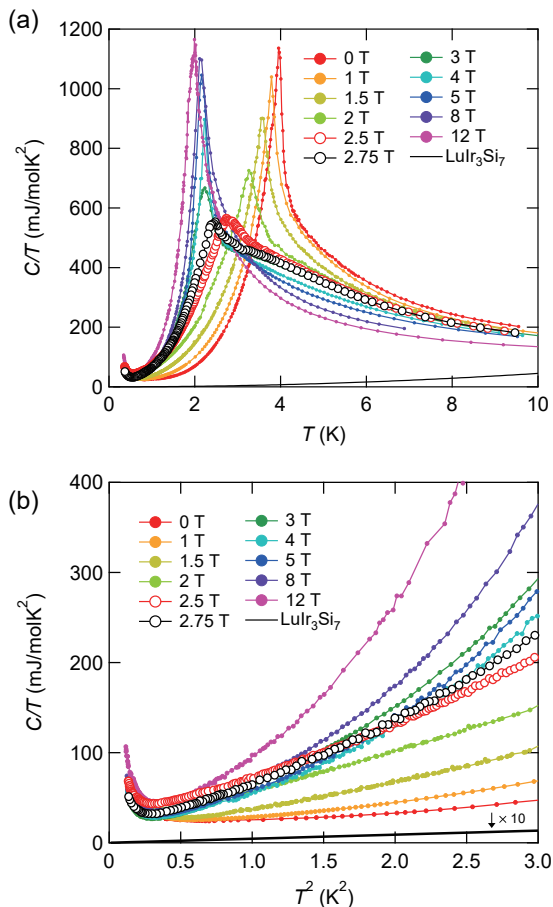


FIG. 2: (a) Temperature dependence of the specific heat divided by temperature $C(T)/T$ of YbIr_3Si_7 in magnetic field perpendicular to the ab plane. Solid line represent $C(T)/T$ of non-magnetic and isostructural LuIr_3Si_7 . (b) $C(T)/T$ vs. T^2 at low temperatures in the magnetically ordered states.

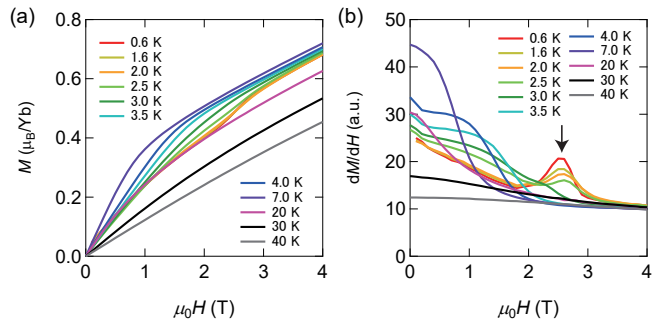


FIG. 3: (a) Field dependence of the magnetization M for $\mathbf{H} \parallel c$. (b) Field dependence of dM/dH . Peak indicated by the arrow corresponds to the boundary between AF-I and AF-II phases.

B. Phase diagram

Figure 2(a) displays the T -dependence of the specific heat divided by temperature, $C(T)/T$ of crystal #1 in zero and finite magnetic fields applied for $\mathbf{H} \parallel c$. Below 10 K, $C(T)/T$ increases gradually with decreasing T and shows a very sharp peak at $T_N = 4.0$ K in zero field. As indicated by arrows in Fig. 1(c), the resistivity shows an anomaly at around T_N determined by the specific heat. This temperature dependence of C/T is similar to that reported in metallic CeRhIn_5 that undergoes an AFM transition [27]. The enhancement of the specific heat above T_N might indicate the importance of short-range order. In YbIr_3Si_7 , the magnetic field suppresses the peak height considerably and shifts T_N to lower temperatures. The temperature dependence of C/T changes dramatically at higher fields [23]. Above $\mu_0 H \approx 3$ T, $C(T)/T$ again exhibits a sharp peak, and the peak height increases rapidly, followed by a nearly saturated behavior above $\mu_0 H = 5$ T. In contrast to lower fields, T_N is nearly independent of applied magnetic field. Figure 2(b) depicts C/T plotted as a function of T^2 at low temperatures. An upturn of $C(T)/T$ at very low temperature ($T \lesssim 0.6$ K) is attributed to the Schottky anomaly.

The specific heat data clearly indicate the presence of two distinct AFM phases, i.e., low-field AF-I and high-field AF-II phases. To determine the phase boundary between these two phases below T_N , we measured the H -dependence of the magnetization M for $\mathbf{H} \parallel c$, as shown in Fig. 3(a). At around $\mu_0 H \approx 2.5$ T, $M(H)$ curves show inflection points at low temperatures. To see this more clearly, we plot the field derivative of the magnetization dM/dH in Fig. 3(b). At low temperatures, dM/dH shows a distinct peak as a function of H , which is attributed to the phase transition between AF-I and AF-II phases. The peak field of dM/dH is independent of temperature. In addition, no discernible hysteresis is observed between up-sweep and down-sweep magnetization measurements. Therefore, AF-I and AF-II phases are likely separated by a weak first-order phase transition.

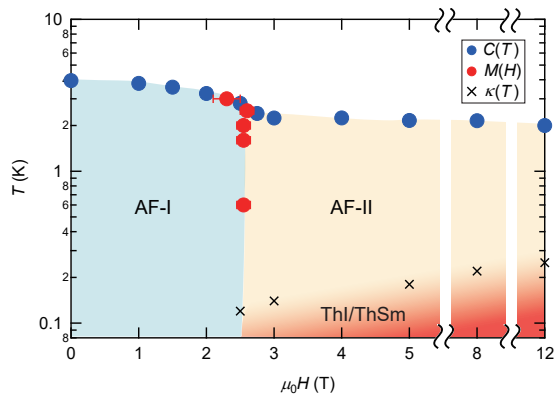


FIG. 4: H - T phase diagram of YbIr_3Si_7 for $\mathbf{H} \parallel c$ axis determined by the specific heat and magnetization. The Néel temperatures (filled blue circles) are determined by the peak temperature of $C(T)/T$ and phase boundary (red filled circles) is determined by the peak of dM/dH . In the AF-I phase, the spins are oriented along the c axis. The AF-II phase is in the spin-flop phase, where the spins are oriented in the ab plane. The crosses represent the temperatures at which gap formation occurs, which is determined by the deviation of κ/T from T^2 -dependence shown by arrows in Figs. 8(d)-(h). The red colored regime represents thermal insulator or thermal semi-metal (ThI/ThSm) regime.

Figure 4 displays the H - T phase diagram for $\mathbf{H} \parallel c$ axis determined by the specific heat and magnetization measurements. The Néel temperatures are determined by the peak temperature of $C(T)/T$. To obtain information on the nature of the phase transition, we performed nuclear magnetic resonance (NMR) measurements for $\mathbf{H} \parallel c$. Figures 5(a) and (b) depict the magnetic-field swept ^{29}Si -NMR spectrum in the AF-I and AF-II phases, respectively. There are two crystallographically inequivalent Si sites, Si(1) and Si(2), as illustrated in Fig. 1(a). For comparison, the NMR spectrum at 4.2 K above T_N are also shown by gray dotted lines. In the AF-I phase, the NMR spectrum splits into three peaks. The peaks in the higher and lower magnetic fields indicate that an internal magnetic field at the Si(2) site is parallel to the external magnetic field, which is shown in the inset of Fig. 5(a). This spin structure is consistent to that reported by neutron diffraction measurements. The middle peak arises from the Si(1) site at which an internal magnetic field from the Yb magnetic moment is canceled. On the other hand, in the AF-II phase, only one peak is observed. This peak slightly shifts to a lower field below T_N . This small shift suggests that dominant magnetic moments are oriented perpendicular to the external magnetic field, as shown in the inset of Fig. 5(b), although the tilted angle from the ab plane cannot be determined precisely in the present measurements. Thus the NMR experiment reveals the spin-flop transition in which the magnetic moments oriented along the c axis in the AF-I phase are rotated to the ab plane in the AF-II phase.

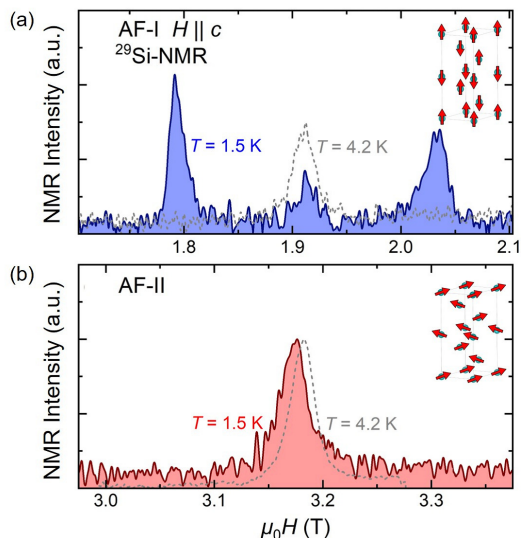


FIG. 5: Magnetic-field swept ^{29}Si -NMR spectrum (a) in the AF-I phase and (b) in the AF-II phase. Gray dotted lines represent the NMR spectrum at 4.2 K (paramagnetic state). In the AF-I phase, the NMR spectrum splits into three peaks, while in the AF-II phase, only one peak is observed. The NMR results indicate the spin-flop transition. The expected magnetic structure in each phase is shown in the insets.

III. GAPLESS EXCITATIONS IN THE INSULATING STATE

A. Specific heat

The specific heat of nonmagnetic and isostructural LuIr_3Si_7 is plotted in Figs. 2(a) and 2(b) to estimate the phonon contribution. The phonon specific heat is negligibly small in the whole temperature range. As shown in Fig. 2(b), $C(T)/T$ at low temperatures varies rapidly with T at high fields. As the field is lowered, the T -dependence becomes weaker. Except for the very low T -regime, where $C(T)/T$ shows an upturn due to the Schottky anomaly, $C(T)/T$ increases with upward curvature with increasing T .

Figures 6(a)-(h) display $C(T)/T$ vs. T^2 at low temperatures. Obviously, the extrapolation of $C(T)/T$ above 1 K to $T = 0$ yields finite intercepts for all fields, indicating the presence of a finite γ . As shown in these figures, the specific heat can be fitted by

$$\frac{C(T)}{T} = \gamma + \beta_M T^\alpha + \frac{C_{Sch}(T)}{T}, \quad (1)$$

for all fields. Here, α is the exponent of power-law temperature dependence in the second term with the coefficient β_M , and $C_{Sch}(T) = \frac{\Delta^2}{k_B T^2} \frac{e^{\Delta/k_B T}}{(1+e^{\Delta/k_B T})^2}$ is the two-level nuclear Schottky term, where Δ is the corresponding energy splitting. As seen in Fig. 2(b), C/T increases steeper than $C/T \propto T^2$ line in the whole field range, indicating that α is larger than 2. The AFM spin-wave

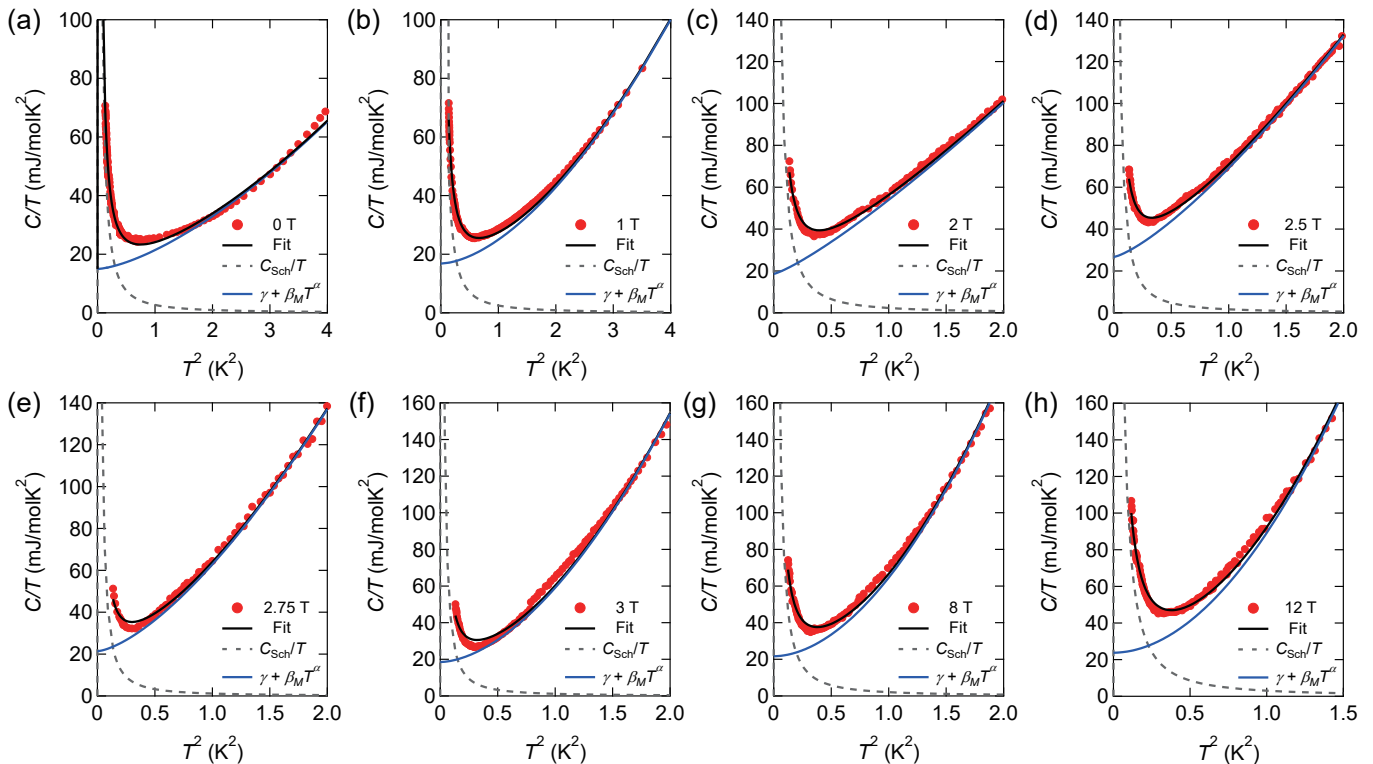


FIG. 6: (a)-(h) C/T vs. T^2 at several fields at low temperatures. The black solid, gray dashed and blue solid lines represent the total C/T , Schottky contribution, and $\gamma + \beta_M T^\alpha$ term, respectively, which are obtained by the fitting using Eq. (1).

theory predicts $\alpha = 1$ and 2 for quasi-2D and 3D systems, respectively. Therefore, the results demonstrate the presence of contributions other than spin waves.

In Fig. 7(a), the H -dependence of γ obtained by the fitting of Eq. (1) is shown. In the whole field regime, γ is finite. In the low-field regime, γ is nearly constant. Remarkably, γ is enhanced above ~ 2 T, and peaks in the vicinity of the phase boundary. Upon entering the AF-II phase, γ is first suppressed but then increases gradually with H . To confirm that this H -dependence of γ is not due to a fitting ambiguity, we also plot $C(T)/T$ at 0.7 K, where the Schottky contribution is negligible. The similar H -dependence of $C(0.7\text{K})/T$ indicates that the enhancement of γ near the phase boundary is an intrinsic property. As the system is insulating, finite γ indicates the presence of a finite DOS of charge-neutral excitations. More precisely, the charge-neutral quasiparticle excitations in the AF-I and II phases are either gapless or gapped with an extremely small excitation energy gap, much smaller than 0.7 K. We shall discuss this issue in more detail below.

The strong suppression of the peak height of $C(T)/T$ and the reduction of T_N with approaching the phase boundary between the AF-I and AF-II phases suggest a possible influence from a putative field-induced AFM quantum critical point (QCP). In fact, the magnitude of the magnetic moment is expected to be strongly reduced with approaching an AFM QCP, which leads to

the suppression of the peak height of the specific heat, as reported in CeRhIn_5 [27]. In YbIr_3Si_7 , however, the putative AFM QCP is avoided by a transition into the AF-II phase. Nevertheless, the quantum critical fluctuations emanating from an avoided QCP in the AF-II phase would lead to the reduction of the magnetic moment. These results lead us to consider that the enhancement of γ in the AF-I phase near the phase boundary is caused by the AFM quantum critical fluctuations. The striking enhancement of γ near the AFM QCP has been reported in several classes of strongly correlated electron systems, including heavy fermions [27] and iron pnictides [28]. The present results suggest that fluctuations emanating from an avoided AFM QCP largely modify the DOS of the neutral fermions.

B. Thermal conductivity

The specific heat involves both localized and itinerant excitations. Therefore, a finite γ does not always indicate the presence of mobile gapless excitations. In fact, amorphous solids and spin glasses exhibit a finite γ , although the excitations in these systems are localized. Moreover, the Schottky anomaly in the specific heat often prevents the analysis of C at very low temperatures. In contrast, the thermal conductivity is determined exclusively by itinerant excitations. In addition, it is free

from the Schottky anomaly, enabling us to extend the measurements down to lower temperatures. In particular, a finite intercept κ_0/T provides the most direct and compelling evidence for the presence of the itinerant and gapless fermionic excitations, analogous to the excitations near the Fermi surface in pure metals.

Figures 8(a)-(h) show κ/T of crystal #1 plotted as a function of temperature in zero and finite magnetic fields for $\mathbf{H} \parallel c$ at very low temperatures. In the AF-I phase, the temperature slope of κ/T decreases continuously with decreasing temperature. We find that κ/T for $\mu_0 H = 0, 1, \text{ and } 2 \text{ T}$ is well fitted as $\kappa/T = \kappa_0/T + c_1 T^p$ (c_1 is a constant) with $p = 1.3, 1.55, \text{ and } 1.74$, as shown by the solid straight lines in the insets of Figs. 8(a), (b), and (c). As shown in Figs. 8(d)-(h), the behavior of the thermal conductivity in the AF-II phase at $\mu_0 H \geq 2.5 \text{ T}$ is fundamentally different from that in the AF-I phase; the temperature dependence of κ/T shows a concave downward curvature below $\sim 0.3 \text{ K}$. As shown by dashed lines in the insets of Figs. 8(d)-(h), κ/T increases nearly proportional to T^2 in the high-temperature regime. At very low temperatures, κ/T deviates from the T^2 -dependence.

In insulating systems, the thermal conductivity can be written as a sum of the phonon and non-phononic quasiparticle contributions, $\kappa = \kappa_{ph} + \kappa_{qp}$. We first discuss the phonon contribution to the total thermal conductivity. When the mean free path of acoustic phonons ℓ_{ph} exceeds the average size of the samples at low tempera-

tures, the phonons undergo specular or diffuse scattering from crystal boundaries. The phonon conductivity in the boundary-limited scattering regime at low temperature is expressed as $\kappa_{ph} = \frac{1}{3} \beta_{ph} \langle v_s \rangle \ell_{ph} T^3$, where β_{ph} is the phonon specific heat coefficient ($C_{ph} = \beta_{ph} T^3$), and $\langle v_s \rangle$ is the mean acoustic phonon velocity. For diffuse scattering, ℓ_{ph} becomes T -independent, resulting in $\kappa_{ph} \propto T^3$. On the other hand, in the case of specular reflection, ℓ_{ph} follows a T^{-1} -dependence, leading to $\kappa_{ph} \propto T^2$. In real systems, $\kappa_{ph} \propto T^a$ with a of intermediate value between 2 and 3. Since the temperature dependence of κ/T in the low temperature regime of the AF-II phase shown in Figs. 8(d)-(h) is expressed as $\kappa/T \propto T^q$ with q less than unity, it cannot be explained by the phonon conductivity. As shown in the inset of Fig. 8(h), the T^2 coefficient of κ/T in the high temperature regime at $\mu_0 H = 12 \text{ T}$ is very small, indicating negligibly small phonon thermal conductivity. The spin-phonon scattering reduces the phonon mean free path. As the magnetic field tends to align the spin direction, the spin-phonon scattering is reduced at high magnetic fields. Therefore, the results of κ/T at 12 T provides an upper limit of the phonon contribution. Thus these considerations indicate that the phonon contribution to the total thermal conductivity is negligibly small at low temperatures, i.e. the thermal conductivity is dominated by non-phononic quasiparticles ($\kappa \approx \kappa_{qp}$).

In zero field, the linear extrapolation of κ/T to $T = 0$ has almost a zero intercept, indicating a zero or vanishingly small value of $\kappa_0/T \lesssim 1 \text{ mW/K}^2\text{m}$. On the other hand, the extrapolation to $T = 0$ has finite intercepts for $\mu_0 H = 1$ and 2 T , yielding $\kappa_0/T \approx 6 \pm 1$ and $8 \pm 1 \text{ mW/K}^2\text{m}$, respectively. These results demonstrate the presence of mobile and gapless fermionic excitations in the AF-I phase. We stress that the observed finite κ_0/T does not originate from charged quasiparticles, in contrast to conventional metals. Evidence for this is provided by the spectacular violation of the Wiedemann-Franz (WF) law, which connects the electronic thermal conductivity κ^e to the electrical resistivity ρ . In metals at low temperatures, the ratio $L = \kappa^e \rho / T \leq L_0$ is satisfied, where $L_0 = (\pi^2/3)(k_B/e)^2 = 2.44 \times 10^{-8} \text{ W}\Omega\text{K}^{-2}$ is the Lorenz number. The values of $\kappa_0 \rho_0 / T$, where ρ_0 is the residual resistivity, are found to be $\sim 2.6 \times 10^3 L_0$ and $\sim 3.5 \times 10^3 L_0$ at $\mu_0 H = 1$ and 2 T , respectively. Here we used $\kappa_0/T = 6.4$ and $8.6 \text{ mW/K}^2\text{m}$ at $\mu_0 H = 1$ and 2 T , respectively, and $\rho_0 = 0.99 \Omega\text{cm}$ for both fields. It is highly unlikely that the surface metallic region significantly violates the WF law. In fact, it is well known that the WF law holds in the 2D metals, even in the quantum Hall regime. We also note that the WF expectation of L_0/ρ_0 from the metallic surface is less than $2.5 \times 10^{-3} \text{ mW}\Omega\text{K}^{-2}\text{m}^{-1}$, which is by far smaller than the experimental resolution. These results lead us to conclude that the neutral fermions in the insulating bulk state are responsible for the observed finite κ_0/T . This suggests that, as the bulk resistivity diverges as $T \rightarrow 0$, the Lorenz number for the heat-carrying quasiparticles

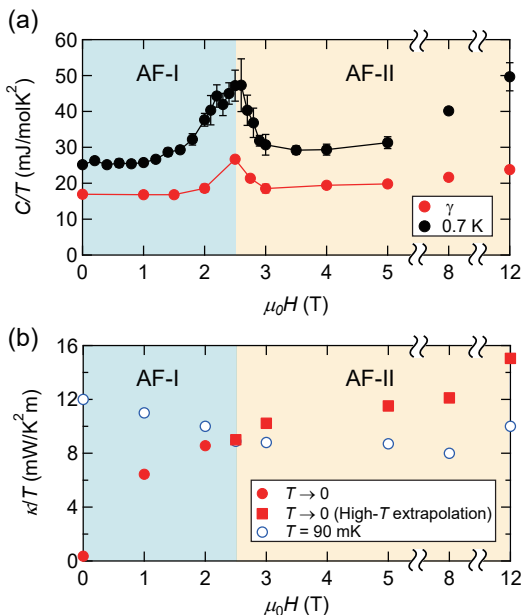


FIG. 7: (a) Field dependence of γ , which is obtained by the fitting using Eq. (1) (see Figs. 6(a)-(h)), and C/T at 0.7 K . (b) Field dependence of the residual thermal conductivity κ_0/T (red filled circles) in the AF-I phase and κ/T obtained by the extrapolation from high temperature regimes to $T = 0$ in the AF-II phase (red filled squares). Open blue circles represent κ/T at 90 mK .

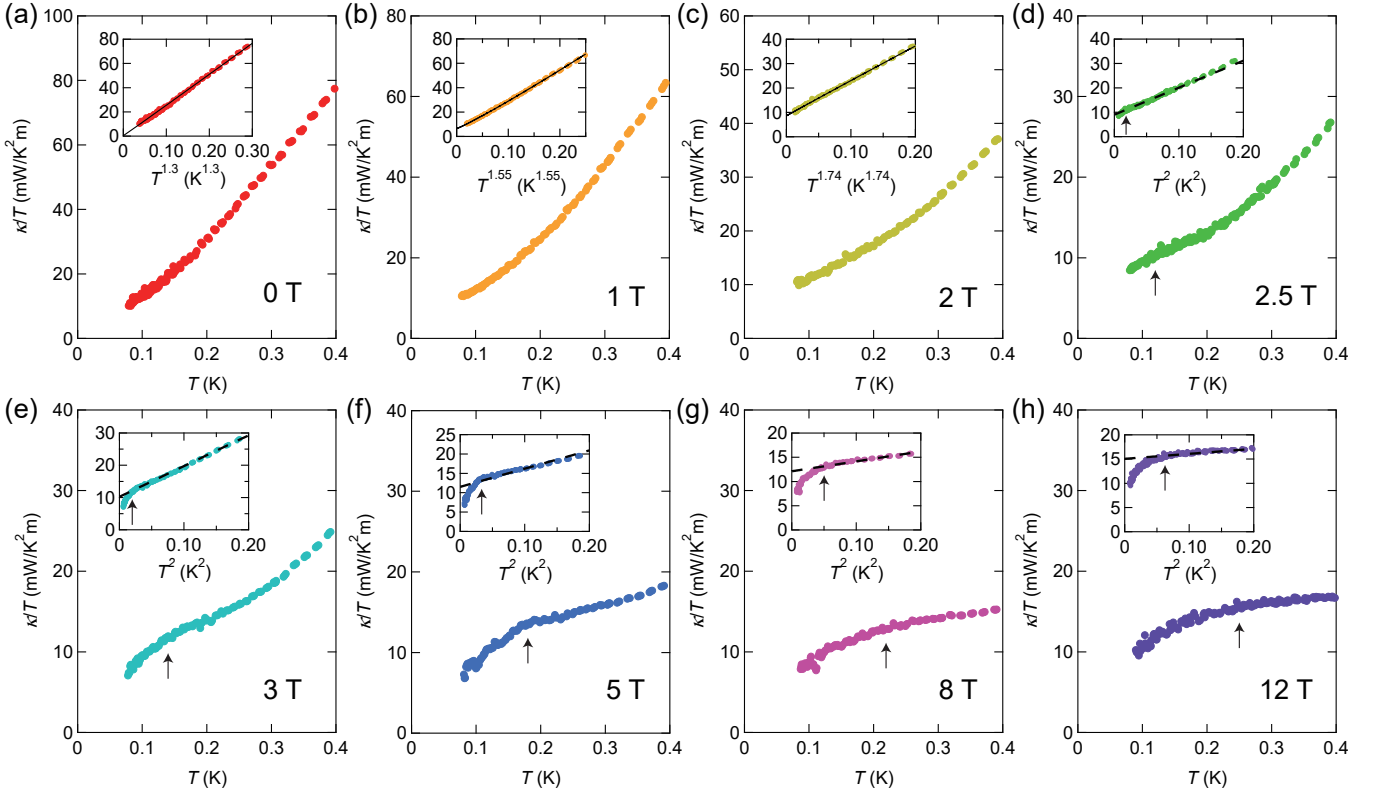


FIG. 8: (a)-(h) Thermal conductivity divided by temperature κ/T versus T in zero and magnetic field for $\mathbf{H} \parallel c$ at very low temperatures. The insets of (a), (b) and (c) show κ/T plotted as a function of T^p with $p=1.3, 1.55$ and 1.74 , respectively. The insets of (d)-(h) show κ/T vs. T^2 . The solid straight lines of (a)-(c) represent the results of the fitting. The dashed straight lines in (d)-(h) represent the linear extrapolation from the high temperature regimes. Arrows in the main panels and insets indicate the temperatures at which κ/T deviates from the T^2 -dependence.

also diverges. Thus, the thermal conductivity and heat capacity data under magnetic fields in the AF-I phase of YbIr_3Si_7 provide evidence for the presence of highly mobile and gapless neutral fermion excitations, which has been similarly reported in YbB_{12} .

We note parenthetically that finite values of both γ and κ_0/T in the insulating states have been reported in quantum-spin-liquid candidates with 2D triangular lattices, including the organic compounds, $\text{EtMe}_3\text{Sb}[\text{Pd}(\text{dmit})_2]_2$ [29] and $\kappa\text{-H}_3(\text{Cat-EDT-TTF})_2$ [30], and inorganic compounds, $1T\text{-TaS}_2$ [31] and $\text{Na}_2\text{BaCo}(\text{PO}_4)_2$ [32]. In $\text{EtMe}_3\text{Sb}[\text{Pd}(\text{dmit})_2]_2$, although the presence or absence of finite κ_0/T has been controversial among different research groups [33, 34], it has been shown very recently that differences between data sets are likely to be due to the cooling rate [35]. In $1T\text{-TaS}_2$, as finite κ_0/T readily disappears by the introduction of disorder/impurity, the magnitude of κ_0/T appears to depend strongly on the sample quality [31]. These results suggest that high-quality single crystals are required to observe the finite κ_0/T in quantum spin liquid systems. In the above compounds, finite γ and κ_0/T have been discussed in terms of electrically neutral spinons forming the Fermi surface.

In the AF-II phase of YbIr_3Si_7 , as shown by the dashed

lines in the insets of Figs. 8(e)-(h), the linear extrapolation of κ/T from the high-temperature regime has finite intercepts at $T = 0$. However, remarkable deviations from the T^2 -dependence and suppression of κ/T at very low temperatures are clearly observed, likely indicating an opening of a tiny gap in the spectrum of the itinerant excitations. As this gap formation occurs below $\sim 0.3\text{ K}$, the estimate of the gap is two orders of magnitude smaller than the Kondo gap ($\sim 60\text{ K}$). We point out that there are two possible explanations for this behavior at very low temperatures well below $\sim 0.3\text{ K}$. One is a fully gapped thermal insulating state and the other is thermal semimetallic or nodal metallic state with a linearly vanishing DOS, as indicated by red shaded regime in Fig. 4. To clarify which scenario is realized, future measurements at lower temperature are required.

We note that the specific heat measurements cannot resolve this gap formation due to the Schottky anomaly. The red filled circles in Fig. 7(b) represent κ_0/T in the AF-I phase. After the initial rapid increase, κ_0/T increases slowly. In Fig. 7(b), $\kappa/T(T \rightarrow 0)$ in the AF-II phase, which is obtained by the linear extrapolation from the high-temperature regime to $T=0$, is plotted by filled red squares. For comparison, we also plot κ/T at 90 mK . Interestingly, κ/T obtained by high-temperature extrap-

olation appears to lie on top of the extrapolation from the AF-I phase. This suggests that κ_0/T steadily increases with magnetic field, but is strongly affected by the spin-flop transition. This field dependence indicates that the itinerant neutral fermions couple to the magnetic field and are strongly influenced by the magnetic ordering.

IV. DISCUSSION

The combined results of the specific heat and thermal conductivity provide pivotal information on the neutral fermions observed in insulating materials. As shown by Figs. 7(a) and 7(b), γ and κ_0/T exhibit very different H -dependence. In particular, at zero field, while γ is finite, no sizable κ_0/T is observed. We note that the result at zero field bears a resemblance to that of SmB_6 . On the other hand, finite γ and κ_0/T values in YbB_{12} are similar to those of YbIr_3Si_7 in a finite field in the AF-I phase. In YbB_{12} , the γ value is nearly sample independent, while κ_0/T values are strongly sample dependent, which is attributed to the amount of the impurities/defects determining the mean free path of the quasiparticles. In contrast, in the present study, we find strong field dependence of κ_0/T in a single sample, which cannot be due to the change in the impurity scattering. The rapid enhancement of κ_0/T at low H is attributed to the increase of the number of mobile heat carriers and/or the change of the dispersion of the neutral particles, which results in the increase of the group velocity. The absence of an enhancement of κ_0/T near the avoided QCP, despite the enhancement of γ , may be because κ_0/T is proportional to $\gamma\tau$, where τ is the scattering time. To explain why κ_0/T is not seriously affected by the enhancement of γ near the QCP, it is required that τ is inversely proportional to the DOS of the neutral fermions, $\tau \propto 1/\gamma$. Such a mechanism is, for example, observed in d -wave superconducting materials, which show an universal residual thermal conductivity [36].

The nature and behavior of the novel charge neutral fermions are not well understood; there are very few experimental results that can be used as tests of the various theoretical models, which include 3D Majorana fermions, composite magnetoexcitons, and spinons in fractionalized Fermi liquids. In this sense, our observations that the itinerant neutral fermions are very sensitive to the magnetic ordering can put significant restrictions on the various theories. The tiny gap formation (or a linearly vanishing DOS) in the AF-II phase indicates a transition from a thermal metal into an insulator (or a thermal semimetal), while the material remains an electrical insulator. This result demonstrates that the Fermi surface of the charge-neutral fermions becomes unstable towards gap formation at low temperatures, which is driven by the magnetic transition of the insulator. Therefore it is natural to consider that the neutral fermions are

composed of strongly magnetically coupled c and f electrons through the Kondo effect. In this situation, neutral fermion excitations will be affected by AFM order and fluctuations.

V. CONCLUSIONS

In summary, we performed specific heat, thermal conductivity and NMR measurements of bulk insulating YbIr_3Si_7 at low temperatures. In the low-field AF-I phase, we find finite γ and κ_0/T , demonstrating the emergence of itinerant gapless excitations. A spectacular violation of the Wiedemann-Franz law directly indicates that YbIr_3Si_7 is a charge insulator but a thermal metal. More precisely, the charge-neutral quasiparticle excitations are either gapless or gapped with an extremely small excitation energy gap, much smaller than the base temperature 90 mK of our thermal conductivity measurements. A spin-flop transition is revealed by NMR measurements. With approaching the spin-flop transition, γ is largely enhanced. Remarkably, inside the high-field AF-II phase, κ/T exhibits a sharp drop at very low temperatures, indicating the opening of a tiny gap much smaller than the Kondo gap or a linear vanishing DOS of the neutral excitations. This demonstrates a field-induced transition from a thermal metal into an insulator/semimetal driven by the spin-flop transition. The present results demonstrate that the neutral fermions are directly coupled to the spin degrees of freedom. Moreover, the Fermi surface of the neutral fermions has an instability towards a novel gapped or semimetallic state. Our experimental observations impose a strong constraint on the theories of charge-neutral fermions. Thus YbIr_3Si_7 provides an intriguing platform for studying the neutral fermions in strongly correlated insulators.

ACKNOWLEDGMENTS

A.H.N. and E.M. acknowledge fruitful discussions with Chris Hooley. Y.M. acknowledges discussion with H. Kontani, Lu Li, and J. Singleton. A.H.N. was supported by the National Science Foundation grant No. DMR-1917511 and the Robert A. Welch Foundation grant C-1818. This work is supported by Grants-in-Aid for Scientific Research (KAKENHI) (Nos. JP15H02106, JP18H01177, JP18H01178, JP18H01180, JP18H05227, JP19H00649, JP20H02600, JP18K03511 and JP20H05159) and on Innovative Areas ‘‘Quantum Liquid Crystals’’ (No. JP19H05824) from Japan Society for the Promotion of Science (JSPS), and JST CREST (JPMJCR19T5). GC acknowledges the support from NSF via grant DMR 1903888.

- [1] T. Takabatake *et al.* *Ce- and Yb-based Kondo semiconductors*, J. Magn. Magn. Mater. **177-181**, 277 (1998).
- [2] P. S. Riseborough, *Heavy fermion semiconductors*, Adv. in Phys. **49**, 257 (2000).
- [3] G. Li, Z. Xiang, F. Yu, T. Asaba, B. Lawson, P. Cai, C. Tinsman, A. Berkley, S. Wolgast, Y. S. Eo, D. J. Kim, C. Kurdak, J. W. Allen, K. Sun, X. H. Chen, Y. Y. Wang, Z. Fisk, L. Li, *Two-dimensional Fermi surfaces in Kondo insulator SmB_6* . Science **346**, 1208 (2014).
- [4] B. S. Tan, Y. T. Hsu, B. Zeng, M. Ciomaga Hatnean, N. Harrison, Z. Zhu, M. Hartstein, M. Kiourlappou, A. Srivastava, M. D. Johannes, T. P. Murphy, J. H. Park, L. Balicas, G. G. Lonzarich, G. Balakrishnan, S. E. Sebastian, *Unconventional Fermi surface in an insulating state*, Science **349**, 287 (2015).
- [5] Z. Xiang, Y. Kasahara, T. Asaba, B. Lawson, C. Insman, LuChen, K. Sugimoto, S. Kawaguchi, Y. Sato, G. Li, S. Yao, Y. L. Chen, F. Iga, J. Singleton, Y. Matsuda, L. Li, *Quantum oscillations of electrical resistivity in an insulator*, Science **69**, 65 (2018).
- [6] M. Hartstein, W. H. Toews, Y. T. Hsu, B. Zeng, X. Chen, M. Ciomaga Hatnean, Q. R. Zhang, S. Nakamura, A. S. Padgett, G. Rodway-Gant, J. Berk, M. K. Kingston, G. H. Zhang, M. K. Chan, S. Yamashita, T. Sakakibara, Y. Takano, J. H. Park, L. Balicas, N. Harrison, N. Shitsevalova, G. Balakrishnan, G. G. Lonzarich, R. W. Hill, M. Sutherland, S. E. Sebastian, *Fermi surface in the absence of a Fermi liquid in the Kondo insulator SmB_6* , Nat. Phys. **14**, 166 (2018).
- [7] Z. Xiang, L. Chen, K.-W. Chen, C. Tinsman, Y. Sato, T. Asaba, H. Lu, Y. Kasahara, M. Jaime, F. Balakirev, F. Iga, Y. Matsuda, J. Singleton, L. Li, *Unusual high-field metal in a Kondo insulator*, Nat. Phys. (to be published), arXiv:2102.13311.
- [8] Y. Sato, Z. Xiang, Y. Kasahara, T. Taniguchi, S. Kasahara, L. Chen, T. Asaba, C. Tinsman, H. Murayama, O. Tanaka, Y. Mizukami, T. Shibauchi, F. Iga, J. Singleton, L. Li, Y. Matsuda, *Unconventional thermal metallic state of charge-neutral fermions in an insulator*, Nat. Phys. **15**, 954 (2019).
- [9] T. T. Terashima, Y. H. Matsuda, Y. Kohama, A. Ikeda, A. Kondo, K. Kindo, F. Iga, *Magnetic-Field-Induced Kondo Metal Realized in YbB_{12}* , Phys. Rev. Lett. **120**, 257206 (2018).
- [10] M. E. Boulanger, F. Laliberté, M. Dion, S. Badoux, N. Doiron-Leyraud, W. A. Phelan, S. M. Koohpayeh, W. T. Fuhrman, J. R. Chamorro, T. M. McQueen, X. F. Wang, Y. Nakajima, T. Metz, J. Paglione, L. Taillefer, *Field-dependent heat transport in the Kondo insulator SmB_6 : Phonons scattered by magnetic impurities*, Phys. Rev. B. **97**, 245141 (2018).
- [11] Y. Xu, S. Cui, J. K. Dong, D. Zhao, T. Wu, X. H. Chen, K. Sun, H. Yao, S. Y. Li, *Bulk Fermi Surface of Charge-Neutral Excitations in SmB_6 or Not: A Heat-Transport Study*, Phys. Rev. Lett. **116**, 246403 (2016).
- [12] S. M. Thomas, X. Ding, F. Ronning, V. Zapf, J. D. Thompson, Z. Fisk, J. Xia, P. F. S. Rosa, *Quantum Oscillations in Flux-Grown SmB_6 with Embedded Aluminum*, Phys. Rev. Lett. **122**, 166401 (2019).
- [13] Knolle, J. & Cooper, N. R. *Quantum Oscillations without a Fermi Surface and the Anomalous de Haas-van Alphen Effect*. Phys. Rev. Lett. **115**, 146401 (2015).
- [14] J. Knolle, N. R. Cooper, *Excitons in topological Kondo insulators: Theory of thermodynamic and transport anomalies in SmB_6* , Phys. Rev. Lett. **118**, 096604 (2017).
- [15] D. Chowdhury, I. Sodemann, T. Senthil, *Mixed-valence insulators with neutral Fermi surfaces*, Nat. Commun. **9**, 1766 (2018).
- [16] P. Rao and I. Sodemann, *Cyclotron resonance inside the Mott gap: A fingerprint of emergent neutral fermions*, Phys. Rev. B **100**, 155150 (2019).
- [17] O. Erten, P. Y. Chang, P. Coleman, A. M. Tsvelik, *Skymne Insulators: Insulators at the Brink of Superconductivity*, Phys. Rev. Lett. **119**, 057603 (2017).
- [18] C. M. Varma, *Majoranas in mixed-valence insulators*, Phys. Rev. B. **102**, 155145 (2020).
- [19] H. Shen and L. Fu, *Quantum oscillation from in-gap states and non-Hermitian Landau level problem*, Phys. Rev. Lett. **121**, 026403 (2018).
- [20] R. Peters, T. Yoshida, H. Sakakibara, N. Kawakami, *Coexistence of light and heavy surface states in a topological multiband Kondo insulator*, Phys. Rev. B. **93**, 235159 (2016).
- [21] Y. Tada, *Cyclotron resonance in Kondo insulator*, Phys. Rev. Research **2**, 023194 (2020).
- [22] G. Baskaran, *Majorana Fermi Sea in Insulating SmB_6 : A proposal and a Theory of Quantum Oscillations in Kondo Insulators*, arXiv:1507.03477.
- [23] M. Stavinoha, C.-L. Huang, W. A. Phelan, A. M. Hallas, V. Loganathan, J. W. Lynn, Q. Huang, F. Weickert, V. Zapf, K. R. Larsen, P. D. Sparks, J. C. Eckert, A. B. Puthirath, C. Hooley, A. H. Nevidomskyy, E. Morosan, *Kondo exhaustion and conductive surface states in anti-ferromagnetic YbIr_3Si_7* , arXiv:1908.11336v2.
- [24] M. Dzero, J. Xia, V. Galitski, P. Coleman, *Topological Kondo Insulators*, Annu. Rev. Condens. Matter Phys. **7**, 249 (2016).
- [25] N. Xu, P. K. Biswas, J. H. Dil, R. S. Dhaka, G. Landolt, S. Muff, C. E. Matt, X. Shi, N. C. Plumb, M. Radović, E. Pomjakushina, K. Conder, A. Amato, S. V. Borisenko, R. Yu, H. M. Weng, Z. Fang, X. Dai, J. Mesot, H. Ding, M. Shi, *Direct observation of the spin texture in SmB_6 as evidence of the topological Kondo insulator*, Nat. Commun. **5**, 4566 (2014).
- [26] K. Hagiwara, Y. Ohtsubo, M. Matsunami, S. I. Ideta, K. Tanaka, H. Miyazaki, J. E. Rault, P. Le Fèvre, F. Bertran, A. Taleb-Ibrahimi, R. Yukawa, M. Kobayashi, K. Horiba, H. Kumigashira, K. Sumida, T. Okuda, F. Iga, S. I. Kimura, *Surface Kondo effect and non-trivial metallic state of the Kondo insulator YbB_{12}* . N at. Commun. **7**, 12690 (2016).
- [27] G. Knebel, M.-A. Méasson, B. Salce, D. Aoki, D. Braithwaite, J. P. Brison and J. Flouquet, *High-pressure phase diagrams of CeRhIn_5 and CeCoIn_5 studied by calorimetry*, J. Phys.:Condens. Matter **16**, 8905 (2004).
- [28] T Shibauchi, A Carrington, and Y Matsuda, *A quantum critical point lying beneath the superconducting dome in iron pnictides*, Annu. Rev. Condens. Matter Phys. **5**, 113 (2014).
- [29] M. Yamashita, N. Nakata, Y. Senshu, M. Nagata, H. M. Yamamoto, R. Kato, T. Shibauchi, and Y. Matsuda, *Highly Mobile Gapless Excitations in a Two-Dimensional*

- Candidate Quantum Spin Liquid*, Science **328**, 1246 (2010).
- [30] M. Shimozawa, K. Hashimoto, A. Ueda, Y. Suzuki, K. Sugii, S. Yamada, Y. Imai, R. Kobayashi, K. Itoh, S. Iguchi, M. Naka, S. Ishihara, H. Mori, T. Sasaki, and M. Yamashita, *Quantum-disordered state of magnetic and electric dipoles in an organic Mott system*, Nat. Commun. **8**, 1821 (2017).
- [31] H. Murayama, Y. Sato, T. Taniguchi, R. Kurihara, X. Z. Xing, W. Huang, S. Kasahara, Y. Kasahara, I. Kimchi, M. Yoshida, Y. Iwasa, Y. Mizukami, T. Shibauchi, M. Konczykowski, and Y. Matsuda, *Effect of quenched disorder on the quantum spin liquid state of the triangular-lattice antiferromagnet 1T-TaS₂*, Phys. Rev. Research **2**, 013099 (2020).
- [32] N. Li, Q. Huang, X. Y. Yue, W. J. Chu, Q. Chen, E. S. Choi, X. Zhao, H. D. Zhou, and X. F. Sun, *Possible itinerant excitations and quantum spin state transitions in the effective spin-1/2 triangular-lattice antiferromagnet Na₂BaCo(PO₄)₂*, Nat. Commun. **11**, 4216 (2020).
- [33] P. Bourgeois-Hope, F. Laliberte, E. Lefrancois, G. Grissonanche, S. R. de Cotret, R. Gordon, S. Kitou, H. Sawa, H. Cui, R. Kato, L. Taillefer, and N. Doiron-Leyraud, *Thermal Conductivity of the Quantum Spin Liquid Candidate EtMe₃Sb[Pd(dmit)₂]₂ : No Evidence of Mobile Gapless Excitations*, Phys. Rev. X **9**, 041051 (2019).
- [34] J. M. Ni, B. L. Pan, B. Q. Song, Y. Y. Huang, J. Y. Zeng, Y. J. Yu, E. J. Cheng, L. S. Wang, D. Z. Dai, R. Kato, and S. Y. Li, *Absence of Magnetic Thermal Conductivity in the Quantum Spin Liquid Candidate EtMe₃Sb[Pd(dmit)₂]₂* Phys. Rev. Lett. **123**, 247204 (2019).
- [35] M. Yamashita, Y. Sato, T. Tominaga, Y. Kasahara, S. Kasahara, H. Cui, R. Kato, T. Shibauchi, and Y. Matsuda, *Presence and absence of itinerant gapless excitations in the quantum spin liquid candidate EtMe₃Sb[Pd(dmit)₂]₂*, Phys. Rev. B **101**, 140407(R) (2020).
- [36] A.V. Balatsky, I. Vekhter, and J.X. Zhu, *Impurity-induced states in conventional and unconventional superconductors*, Rev. Mod. Phys. **78**, 373 (2006).